PERFORMANCE ANALYSIS OF WASTE HEAT RECOVERY WITH A DUAL LOOP ORGANIC RANKINE CYCLE SYSTEM FOR DIESEL ENGINE

Hongjin Wang[1,2]*, Hongguang Zhang[1,2]

[1]College of Environmental and Energy Engineering，Beijing University of Technology，Pingleyuan No.100, 100124 Beijing, China
[2]Collaborative Innovation Center of Electric Vehicles in Beijing, Pingleyuan No.100, 100124 Beijing, China
e-mail:bjgywanghongjin@163.com

* Corresponding Author

ABSTRACT

To take full advantage of the waste heat from a diesel engine, a set of dual loop organic Rankine cycle system (ORCs) was designed to recover exhaust energy, waste heat from the coolant system, and released heat from turbocharged air in the intercooler of a six-cylinder diesel engine. Aspen plus software was used to model the dual loop ORCs. According to the simulation model, the operating performance of the dual loop ORCs and the fuel economy of the diesel engine were investigated. The results show that the thermodynamic performance and economy performance of the diesel engine can be effectively improved by using the dual loop ORCs. At the engine rated condition, the overall net power output of the dual loop ORCs is up to 43.65 kW. The brake specific fuel consumption (BSFC) and the thermal efficiency of the diesel engine-dual loop ORCs are 191.24 $g\cdot(kW\cdot h)^{-1}$ and 37.57%, respectively. Compared with the diesel engine, the thermal efficiency of the combined system can be increased by 13.69% and the BSFC can be reduced by 15.86%.

1. INTRODUCTION

A large amount of petroleum resources has been consumed by automobiles. Meanwhile, given the low utilization rate for internal combustion engine, the thermal efficiency is only 30%-45% for diesel engine and 20%-30% for gasoline engine. And then the remaining heat is released into the atmosphere (Dolz *et al*., 2012, Roy *et al*., 2010). Therefore, discovering a more effective way to recover internal combustion engine waste heat so as to increase engine thermal efficiency and decrease fuel consumption has become a hot focus of recent research work.

ORCs has been widely used to recover and utilize the low-grade waste heat and recently numerous scholars have investigated the use of ORCs to recover engine exhaust waste heat energy (Fang *et al*.,2010, Liu *et al*., 2012). Shu *et al*. (2014) designed a set of dual loop ORCs to recover exhaust waste heat energy and coolant system waste heat. Results showed that using the dual loop ORCs can effectively improve the thermodynamic performance of the engine. Gao *et al* (2013) proposed ORCs to recover the exhaust waste heat of a turbocharged diesel engine. The results showed that the net power output of the diesel engine can improve 12%. Meinel *et al* (2014) compared a two-stage ORC with internal heat recovery with a simple standard ORCs and an ORC with a recuperator based on Aspen Plus software. The thermodynamic efficiencies of the two-stage cycle exceed the corresponding values of reference ORCs by up to 2.25%.

Although many scholars have analyzed the performance of different kinds of ORCs, most research takes only internal combustion engine exhaust energy into account. Few of them have considered recovering the waste heat from the coolant system, and the released heat from turbocharged air in the intercooler of internal combustion engine. In this paper, a set of dual loop ORCs is designed to recover exhaust waste heat energy, waste heat from the coolant system, and released heat from turbocharged air in the intercooler of a diesel engine. Aspen plus software is used to model the dual loop ORCs, and then the operation performance is analyzed based on the sensitivity analysis under the different high temperature cycle evaporation pressure and the working fluid mass flow rate.

2. MODEL OF DUAL LOOP ORC SYSTEM

2.1 Model of Dual Loop ORCs Based on Aspen Plus

The exhaust temperature of diesel engine is generally high. However, the temperatures of the coolant and the turbocharged air are relatively low. To take full advantage of the waste heat energy from the diesel engine, a set of dual loop ORCs is designed. As shown in Figure 1, the dual loop ORCs contains a high temperature (HT) loop ORCs (the lower part) and a (low temperature) LT loop ORCs (the upper part). The HT loop ORCs is used to recover the high-temperature exhaust energy, while the LT loop ORCs is used to recover the waste heat from the coolant system, the released heat from turbocharged air in the intercooler and the residual heat of low-temperature exhaust energy. Figure 2 and Figure 3 are the *T-s* diagram of the HT loop and LT loop in the dual loop ORCs, respectively.

The dual loop ORCs system operates according to the following process. In the HT loop ORCs (corresponding to Processes 1-7), the working fluid is pressurized into the saturated liquid state working fluid using Pump 1. Then it is preheated in the Recuperator. Subsequently, the working fluid turns into a saturated vapor state in the Evaporator 1. Then, the saturated vapor enters Expander 1 to produce useful work. Finally, the superheated vapor exported from Expander 1 turns into a saturated liquid state after the heat transfer process in the Recuperator and Condenser1. With this change, the HT loop ORCs completes one working cycle. Meanwhile, in the LT loop ORCs (corresponding to Processes 10-16), Pump 2 pressurizes the saturated liquid state working fluid and sends it into the Intercooler to exchange heat with the turbocharged intake air. Then, the working fluid flows into the Preheater and is heated up into the two-phase state by the engine coolant. Later, the two-phase working fluid is heated up into a saturated vapor state by the residual heat of the low-temperature exhaust energy in the Evaporator 2. The saturated vapor enters Expander 2 to make it do work. Finally, the superheated vapor exported from Expander 2 condenses into a saturated liquid state in the Condenser 2. The whole process is then completed.

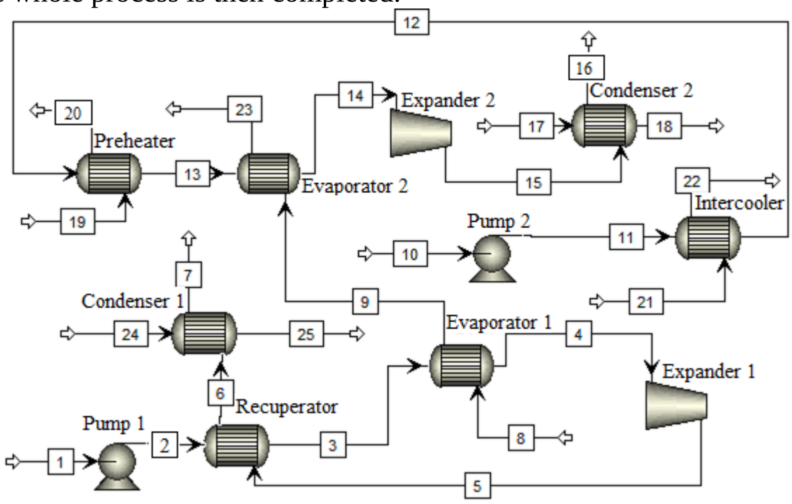

Figure 1: Model of the dual loop ORCs

2.2 Boundary Conditions

(1) The thermodynamic properties of fluid are calculated based on the Peng-Robinson state equation. R123 is selected as the working fluid, water is selected as the coolant. The diesel engine air fuel ratio is set to 19.7, mass fraction of the exhaust components CO_2、H_2O、N_2 and O_2 is 15.1%、5.5%、71.6% and 7.8%, respectively. (Shu *et al*., 2014).

(2) The isentropic efficiencies of expander 1 and expander 2 are both set to 0.7. The isentropic efficiencies of Pump 1 and Pump 2 are both set to 0.65.

(3) The ambient temperature is set to 291.15 K.

(4) The working fluid temperature at the evaporator 1 outlet is set to 456K. When the exhaust

temperature drops below the dew point, the exhaust pipes and evaporator surfaces can erode, so the exhaust temperature at the evaporator 2 outlet is set to 380K. (Bahadori, 2011).
(5) The mass flow rate of the HT loop ORCs is set to 0.4-0.8 kg/s; The evaporation pressure of HT loop ORCs is set to 1.0-2.5MPa.
(6) The cooling water inlet temperature and mass flow rate of Condenser1 are set to 285K and 2kg/s (corresponding to Processes 24-25 in Figure 1); The same as the Condenser2 are set to 285K and 3kg/s (corresponding to Processes 17-18 in Figure 1).
(7) The outlet temperature of engine coolant is set to 340K (corresponding to Processes 21-22 in Figure 1)
(8) The outlet temperature of turbocharged intake air is set to 350K (corresponding to Processes 19-20 in Figure 1)
(9) The test parameters of the diesel engine at rated conditions are listed in Table 1.

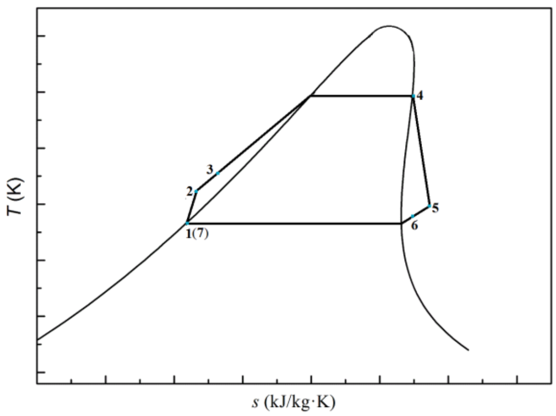

Figure 2: *T-s* diagram of the HT loop ORCs

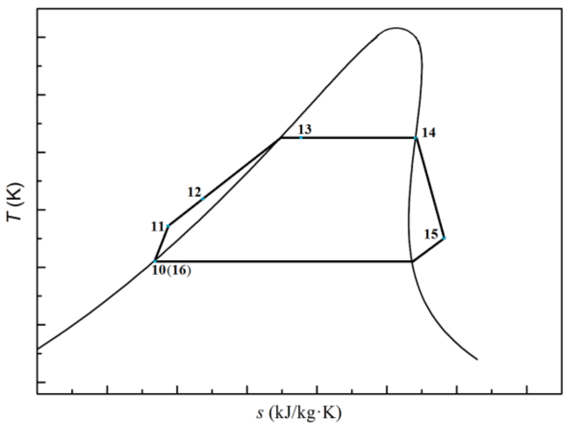

Figure 3: *T-s* diagram of the LT loop ORCs

Table 1: Test parameters of the diesel engine

Items	value
Rated speed/ $r \cdot min^{-1}$	2000
Rated power / kW	275
Exhaust temperature/ K	783
Air intake mass flow rate/ $kg \cdot s^{-1}$	0.43
Fuel consumption/ $kg \cdot h^{-1}$	60.97
Intake air temperature/ K	407
Engine coolant mass flow rate/ $kg \cdot s^{-1}$	1.30
Engine coolant temperature/K	370

2.3 Thermodynamic Model of the Dual Loop ORCs

To evaluate the performance of the dual loop ORCs, the following parameters are selected in the study.

The net power output of HT loop ORCs is given in Equation (1):

$$\dot{W}_{\mathrm{H}} = \dot{W}_{\mathrm{exp1}} - \dot{W}_{\mathrm{p1}} \tag{1}$$

The net power output of LT loop ORCs is given in Equation (2):

$$\dot{W}_{\mathrm{L}} = \dot{W}_{\mathrm{exp2}} - \dot{W}_{\mathrm{p2}} \tag{2}$$

Where $\dot{W}_{\mathrm{p1}}$ and $\dot{W}_{\mathrm{p2}}$ are the power consumed by pump 1 and pump 2, respectively. $\dot{W}_{\mathrm{exp1}}$ and $\dot{W}_{\mathrm{exp2}}$ are the power output of the expander 1 and expander 2, respectively.

The overall net power output of the dual loop ORCs is given in Equation (3):

$$\dot{W}_{\mathrm{oa}} = \dot{W}_{\mathrm{H}} + \dot{W}_{\mathrm{L}} \tag{3}$$

The thermal efficiency of the dual loop ORCs is given in Equation (4):

$$\eta_{\mathrm{oa}} = \frac{\dot{W}_{\mathrm{oa}}}{\dot{Q}_{\mathrm{oa}}} \times 100\% \tag{4}$$

Where $\dot{Q}_{\mathrm{oa}}$ is the overall heat transfer rate of the dual loop ORCs:

$$\dot{Q}_{\mathrm{oa}} = \dot{Q}_{\mathrm{e1}} + \dot{Q}_{\mathrm{e2}} + \dot{Q}_{\mathrm{int}} + \dot{Q}_{\mathrm{pre}} \tag{5}$$

Where $\dot{Q}_{e1}$, $\dot{Q}_{e2}$, $\dot{Q}_{\mathrm{int}}$ and $\dot{Q}_{\mathrm{pre}}$ are the heat transfer rate of evaporator 1, evaporator 2, intercooler and preheater, respectively.

To assess the economy performance of the diesel engine-dual loop ORC combined system, the brake specific fuel consumption (BSFC) of the combined system is defined as:

$$bsfc_{\mathrm{cs}} = \frac{\dot{F}}{\dot{W}_{\mathrm{eng}} + \dot{W}_{\mathrm{oa}}} \times 1000 \tag{6}$$

Where $\dot{F}$ represents the fuel consumption of the diesel engine; $\dot{W}_{\mathrm{eng}}$ represents the power of diesel engine.

The BSFC of the diesel engine is defined as:

$$bsfc_{\mathrm{eng}} = \frac{\dot{F}}{\dot{W}_{\mathrm{eng}}} \times 1000 \tag{7}$$

The improvement ratio of BSFC of the combined system is defined as:

$$\eta_{\mathrm{cs}} = \frac{bsfc_{\mathrm{eng}} - bsfc_{\mathrm{cs}}}{bsfc_{\mathrm{eng}}} \times 100\% \tag{8}$$

The thermal efficiency of the diesel engine is given in Equation (9):

$$\eta_{\mathrm{eng}} = \frac{\dot{W}_{\mathrm{eng}}}{\dot{Q}_{\mathrm{cs}}} \times 100\% \tag{9}$$

Where $\dot{Q}_{\mathrm{cs}}$ represents the overall energy generated by fuel combustion of the diesel engine.

The thermal efficiency of the combined system is defined as:

$$\eta_{\mathrm{cst}} = \frac{\dot{W}_{\mathrm{oa}} + \dot{W}_{\mathrm{eng}}}{\dot{Q}_{\mathrm{cs}}} \times 100\% \tag{10}$$

The increasing ratio of thermal efficiency in the combined system is defined as:

$$\eta_{\mathrm{tei}} = \frac{\eta_{\mathrm{cst}} - \eta_{\mathrm{eng}}}{\eta_{\mathrm{eng}}} \times 100\% \tag{11}$$

The exergy destruction rate of the each components are given in Equations (12)-(22):

$$\dot{I}_{\mathrm{p1}} = T_0 \dot{m}_{\mathrm{H}} (s_2 - s_1) \tag{12}$$

$$\dot{I}_{\mathrm{p2}} = T_0 \dot{m}_{\mathrm{L}} (s_{11} - s_{10}) \tag{13}$$

$$\dot{I}_{\mathrm{r}} = T_0 \dot{m}_{\mathrm{H}} [(s_6 - s_5) + (s_3 - s_2)] \tag{14}$$

$$\dot{I}_{\mathrm{e1}} = T_0 \dot{m}_{\mathrm{H}}[(s_4 - s_3) - \frac{h_4 - h_3}{T_{\mathrm{H,H}}}] \tag{15}$$

Where $T_{\mathrm{H,H}}$ is the temperature of the high temperature heat source in the HT loop ORCs, and is assumed to be equal to $T_{\mathrm{H,H}} = T_4 + 5$.

$$\dot{I}_{\mathrm{e2}} = T_0 \dot{m}_{\mathrm{L}}[(s_{14} - s_{13}) - \frac{h_{14} - h_{13}}{T_{\mathrm{L,H}}}] \tag{16}$$

Where $T_{\mathrm{L,H}}$ is the temperature of the high temperature heat source in the LT loop ORCs, and is assumed to be equal to $T_{\mathrm{L,H}} = T_{14} + 5$.

$$\dot{I}_{\mathrm{exp1}} = T_0 \dot{m}_{\mathrm{H}}(s_5 - s_4) \tag{17}$$

$$\dot{I}_{\mathrm{exp2}} = T_0 \dot{m}_{\mathrm{L}}(s_{15} - s_{14}) \tag{18}$$

$$\dot{I}_{\mathrm{int}} = T_0 \dot{m}_{\mathrm{L}}[(s_{12} - s_{11}) - \frac{h_{12} - h_{11}}{T_{\mathrm{int,H}}}] \tag{19}$$

Where $T_{\mathrm{int,H}}$ is the temperature of the heat source in the intercooler, and is assumed to be equal to $T_{\mathrm{int,H}} = T_{12} + 5$.

$$\dot{I}_{\mathrm{pre}} = T_0 \dot{m}_{\mathrm{L}}[(s_{13} - s_{12}) - \frac{h_{13} - h_{12}}{T_{\mathrm{pre,H}}}] \tag{20}$$

Where $T_{\mathrm{pre,H}}$ is the temperature of the heat source in the intercooler, and is assumed to be equal to $T_{\mathrm{pre,H}} = T_{13} + 5$.

$$\dot{I}_{\mathrm{con1}} = T_0 \dot{m}_{\mathrm{L}}[(s_7 - s_6) - \frac{h_7 - h_6}{T_{\mathrm{H,L}}}] \tag{21}$$

Where $T_{\mathrm{H,L}}$ is the temperature of the low temperature heat source in the HT loop ORCs, and is assumed to be equal to $T_{\mathrm{H,L}} = T_7 - 5$.

$$\dot{I}_{\mathrm{con2}} = T_0 \dot{m}_{\mathrm{L}}[(s_{16} - s_{15}) - \frac{h_{16} - h_{15}}{T_{\mathrm{L,L}}}] \tag{22}$$

Where $T_{\mathrm{L,L}}$ is the temperature of the low temperature heat source in the LT loop ORCs, and is assumed to be equal to $T_{\mathrm{L,L}} = T_{16} - 5$.

Note that Eq. (15),(19),(21)and (22) are derived from Ref. (Yang *et al*., 2014)

3. RESULTS AND DISCUSSION

The variation of the net power output in LT loop ORCs with the evaporation pressure and mass flow rate of the HT loop ORCs is shown in Figure 4. The graph shows that at a certain evaporation pressure of HT loop ORCs, the net power output of the LT loop ORCs decreases gradually with the increase of the mass flow rate of HT loop ORCs. This primarily because that, the heat transfer rate of evaporator 1 increases with the increase of mass flow rate at the HT loop ORCs. Therefore, the heat transfer rate of evaporator 2 decrease. At a certain mass flow rate of HT loop ORCs, the net power output of the LT loop ORCs increases gradually with the increase of the evaporation pressure of HT loop ORCs. When the evaporation pressure and mass flow rate of HT loop ORCs are 2.5 MPa and 0.4 kg·s^{-1} , the net power output of the LT loop ORCs reaches the upper limit and is 24.63 kW.

The variation of the net power output in HT loop ORCs with the evaporation pressure and mass flow rate of the HT loop ORCs is shown in Figure 5. The graph shows that at a certain evaporation pressure of HT loop ORCs, the net power output of the HT loop ORCs increases gradually with the increase of the mass flow rate of HT loop ORCs. At a certain mass flow rate of HT loop ORCs, the net power output of the HT loop ORCs increases gradually with the increase of the evaporation pressure of HT loop ORCs. When the evaporation pressure and mass flow rate of HT loop ORCs are 2.5 MPa and 0.8 kg·s^{-1} , the net power output of the HT loop ORCs reaches the upper limit and is 24.99 kW.

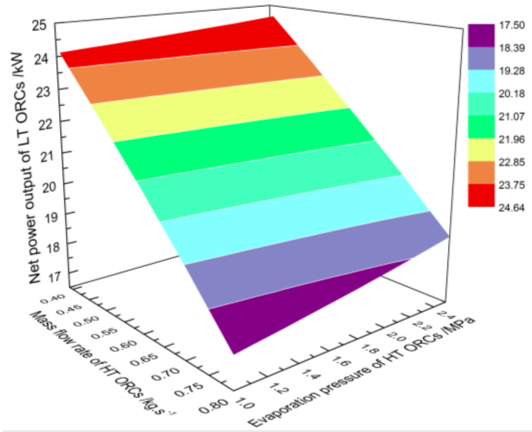

Figure 4: Net power output of the LT loop ORCs

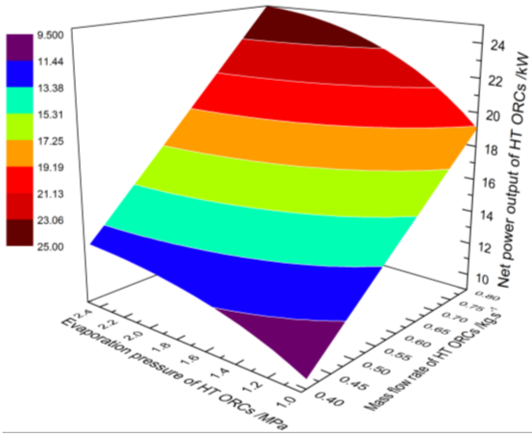

Figure 5: Net power output of the HT loop ORCs

Through the comparison between Figure 4 and Figure 5, it can be concluded that the net power output of the LT loop ORCs and the HT loop ORCs are affected more by mass flow rate of the HT loop ORCs. And the net power output of the LT loop ORC system is greater than that of the HT loop ORC system under the same evaporation pressure of HT ORCs.

The variation of the overall net power output in dual loop ORCs with the evaporation pressure and mass flow rate of the HT loop ORCs is shown in Figure 6. The graph shows that at a certain evaporation pressure of HT loop ORCs, the overall net power output of the dual loop ORCs increases gradually with the increase of the mass flow rate of HT loop ORCs. This primarily because that, with the increase of the mass flow rate of HT loop ORCs, the variation of net power output of HT loop ORCs is relatively higher than that of LT loop ORCs. At a certain mass flow rate of HT loop ORCs, the net power output of the dual loop ORCs increases gradually with the increase of the evaporation pressure of HT loop ORCs. When the evaporation pressure and mass flow rate of HT loop ORCs are 2.5 MPa and 0.8 $kg{\cdot}s^{-1}$, the overall net power output of the dual loop ORCs reaches the upper limit and is 43.65 kW.
The variation of the thermal efficiency in dual loop ORCs with the evaporation pressure and mass flow rate of the HT loop ORCs is shown in Figure 7. Moreover, the thermal efficiency has the same variation tendency with the overall net power output of the dual loop ORCs. The reason can be explained as follows. According to Eq. (4), the thermal efficiency of dual loop ORCs is related to the overall heat transfer rate and the overall net power output of the dual loop ORCs. The overall heat transfer rate is constant due to the constant operating condition of diesel engine, while the overall net power out of dual loop ORCs increases with evaporation pressure and mass flow rate of HT loop ORCs, as shown in Figure 6. When the evaporation pressure and mass flow rate of HT loop ORCs are

2.5 MPa and 0.8 kg·s^{-1}, the thermal efficiency of the dual loop ORCs reaches the upper limit and is 10.52%.

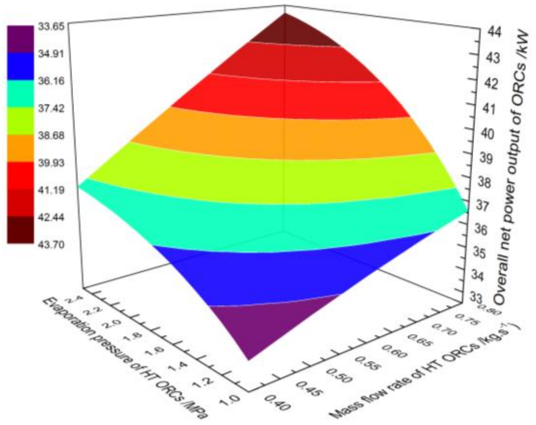

Figure 6: Overall net power output of the dual loop ORCs

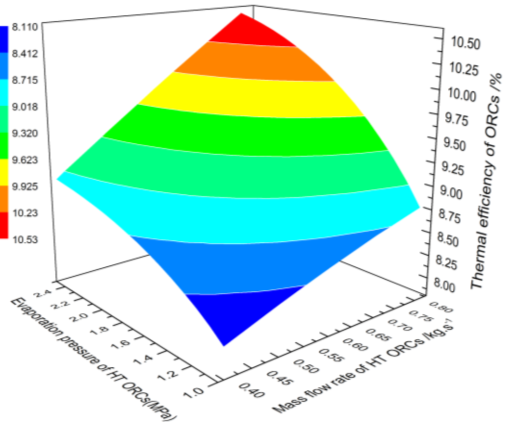

Figure 7: Thermal efficiency of the dual loop ORCs

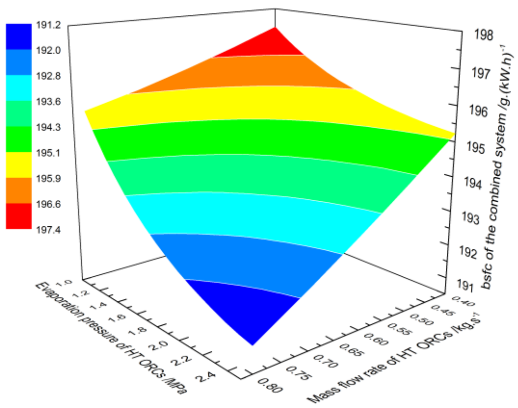

Figure 8: BSFC of the combined system

The variation of the BSFC in diesel engine-dual loop organic Rankine cycle (ORC) combined system with the evaporation pressure and mass flow rate of the HT loop ORCs is shown in Figure 8. The graph shows that at a certain evaporation pressure of HT loop ORCs, the BSFC of the combined system decreases gradually with the increase of the mass flow rate of HT loop ORCs. At a certain mass flow rate of HT loop ORCs, the BSFC of the combined system decreases gradually with the increase of the evaporation pressure of HT loop ORCs. The reason can be explained as follows. According to Eq. (6), the BSFC of combine system is related to the fuel consumption, the power of diesel engine and the overall net power output of the dual loop ORCs. The fuel consumption and the power of diesel engine is constant due to the constant operating condition of diesel engine, while the overall net power out of dual loop ORCs increases with evaporation pressure and mass flow rate of HT loop ORCs, as shown in Figure 4. When the evaporation pressure and mass flow rate of HT loop ORCs are 2.5 MPa and 0.8 $kg{\cdot}s^{-1}$, the BSFC of the diesel engine-dual loop ORC combined system reaches the minimum and is 191.24 $g{\cdot}(kW{\cdot}h)^{-1}$.

The variation of the improvement ratio of BSFC in diesel engine-dual loop ORC combined system with the evaporation pressure and mass flow rate of the HT loop ORCs is shown in Figure 9. The graph shows the improvement ratio of BSFC in the combined system gradually increases with evaporation pressure and mass flow rate of HT loop ORCs. Moreover, the minimum improvement ratio of BSFC is 10.9%. When the evaporation pressure and mass flow rate of HT loop ORCs are 2.5 MPa and 0.8 $kg{\cdot}s^{-1}$, the improvement ratio of BSFC in the diesel engine-dual loop ORC combined system reaches the upper limit and is 13.69%.

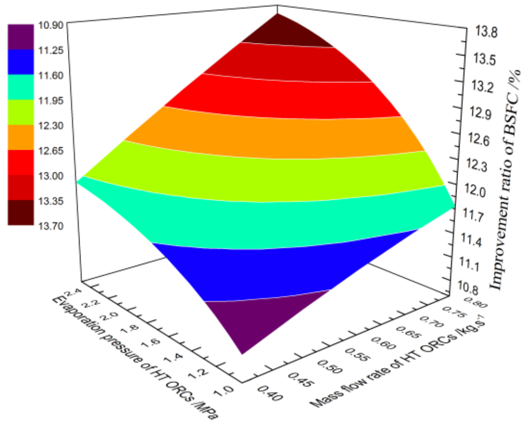

Figure 9: Improvement ratio of BSFC in the combined system

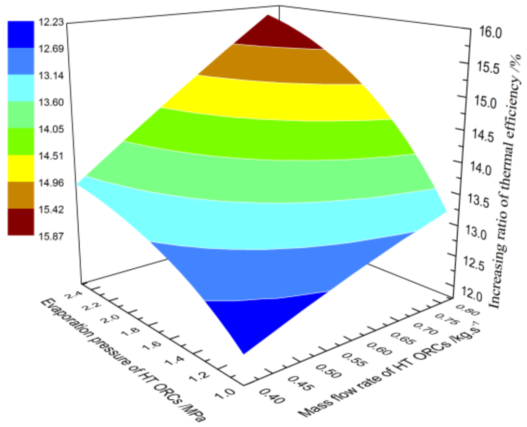

Figure 10: Increasing ratio of thermal efficiency in the combine system

The variation of the thermal efficiency improvement in diesel engine-dual loop ORC combined system with the evaporation pressure and mass flow rate of the HT loop ORCs is shown in Figure 10. Compare with Figure 6, the increasing ratio of thermal efficiency in the combine system has the same variation tendency with the overall net power output of the dual loop ORCs. Moreover, the minimum thermal efficiency improvement is 12.23%. When the evaporation pressure and mass flow rate of HT loop ORCs are 2.5 MPa and 0.8 $kg{\cdot}s^{-1}$, the increasing ratio of thermal efficiency in the diesel engine-dual loop ORC combined system reaches the upper limit and is 15.86%.

Figure 11 shows the variations of the exergy destruction rate in dual loop ORCs under the condition of the overall net power output reaches the upper limit. The graph shows that, the exergy destruction rate of the condenser 2 is bigger than that of other components and is 15.64kW, followed by condenser 1 and evaporator 1. They are 14.70 kW and 13.33 kW, respectively. The exergy destruction of condenser 1 and condenser 2 are all bigger due to the higher temperature difference between the working fluid and cooling water at the condenser. Whereas, the exergy destruction of evaporator 1 is bigger because of the higher temperature difference between the working fluid and exhaust gas at the evaporator 1. The exergy destruction rate of the dual loop ORCs and LT ORCs are 40.78 kW and 29.75 kW, respectively.

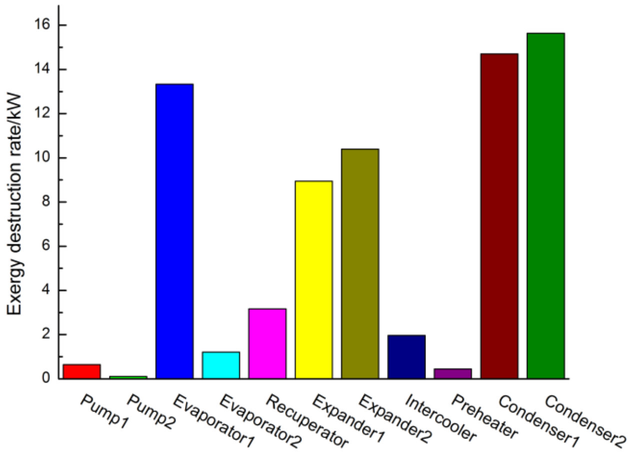

Figure 11: Exergy destruction rate of the dual loop ORCs

4. CONCLUSIONS

- By employing the dual loop ORC system, the waste heat of exhaust energy, coolant system, and released heat from turbocharged air in the intercooler can be effectively recovered and utilized. The overall net power output and thermal efficiency of the dual loop ORCs can reach 43.65kW and 10.52%, respectively.
- The fuel economy of the diesel engine can be notably improved, by employing the dual loop ORCs. When the evaporation pressure and mass flow rate of HT loop ORCs are 2.5 MPa and 0.8 $kg \cdot s^{-1}$, the BSFC of the diesel engine-dual loop ORC combined system is 191.24 $g \cdot (kW \cdot h)^{-1}$, which reduced by 13.69% compared with the diesel engine itself.
- The net power output of LT loop ORCs is greater than that of HT loop ORCs. At the maximum overall net power output condition, the exergy destruction rate of the LT loop ORC system is higher than that of the HT loop ORC system and the difference can reach 11.03kW.

NOMENCLATURE

m	mass flow rate	($kg \cdot s^{-1}$)
h	enthalpy	($kJ \cdot kg^{-1}$)
Q	heat transfer rate	(kJ)
S	entropy	(kJ/kg·K)
T	temperature	(K)
W	work	(kJ)
η	efficiency	(%)
F	fuel consumption	($kg \cdot h^{-1}$)
I	exergy destruction	(kW)

Subscript

1,2, 3…	state point in cycle
H	HT loop ORCs/high temperature heat source
L	LT loop ORCs/low temperature heat source
p	pump
e	evaporator
r	recuperator
exp	expander
int	intercooler
pre	preheater
con	condenser
eng	diesel engine
cs	combined system
oa	overall of dual loop ORCs
cst	thermal efficiency of the combined system
tei	thermal efficiency improvement

REFERENCES

Dolz, V., Novella R., García, A., et al. 2012, HD Diesel engine equipped with a bottoming Rankine cycle as a waste heat recovery system. Part 1: study and analysis of the waste heat energy. *Appl Therm Eng*, vol. 36: p. 269-278.

Roy, J.P., Mishra, M.K., Misra, A., 2010, Parametric optimization and performance analysis of a waste heat recovery system using Organic Rankine Cycle. *Energy*, vol. 35: p. 5049-5062.

Fang, J.L., Wei, M.S., Wang, J.R., et al, 2010, Simulation of Waste Heat Recovery from a Heavy-Duty Diesel Engine with a Medium Temperature ORCs. *Transactions of CSICE*, vol. 4, no. 28: p. 362-367.

Liu, B., Rivière, P., Coquelet, C., et al, 2012, Investigation of a two stage Rankine cycle for electric power plants. *Appl Energ*, vol. 100: p. 285-294.

Tian, H., Liu, L.N., Shu, G.Q., et al, 2014, Theoretical research on working fluid selection for a high-temperature regenerative transcritical dual-loop engine organic Rankine cycle. *Energ Convers Manage*, vol. 86: p. 764-773.

Shu, G.Q., Liu, L.N., Tian.H., et al, 2014, Parametric and working fluid analysis of a dual-loop organic Rankine (DORC) used in engine waste heat recovery. *Appl Energ*, vol. 113: p. 1188-1198.

Gao, W.Z., Zhai, J.M., Li, G.H., et al, 2013, Performance evaluation and experiment system for waste heat recovery of diesel engine. *Energy*, vol.15, no. 55: p. 226-235.

Meinel, D., Wieland, C., Spliethoff, H, 2014, Effect and comparison of different working fluids on a two-stage organic rankine cycle (ORC) concept. *Appl Therm Eng*, vol. 63: p. 246-253.

Yu, G.P., Shu, G.Q., Tian, H. et al. 2013, Simulation and thermodynamic analysis of a bottoming Organic Rankine Cycle. *Energy*, vol. 51: p. 281-290.

Bahadori, A., 2011, Estimation of combustion flue gas acid dew point during heat recovery and efficiency gain. *Appl Therm Eng*, vol. 31: p. 1457-1462.

Yang, F.B., Dong, X.R., Zhang, H.G. et al, 2014, Performance analysis of waste heat recovery with a dual loop organic Rankine cycle (ORC) system for diesel engine under various operating conditions. *Energ Convers Manage*, vol. 80: p. 243-255.

ACKNOWLEDGEMENT

This work was sponsored by the National Natural Science Foundation of China (Grant No. 51376011), the Beijing Natural Science Foundation Program (Grant No. 3152005), and the Scientific Research Key Program of Beijing Municipal Commission of Education (Grant No. KZ201410005003).